

Study of electrical conductivity and hardness of the alloys of ternary Bi-Sb-Zn system and calculation of isothermal section at 298 K

V. Ćosović^{1*}, D. Minić², D. Manasijević³, M. Kolarević⁴, N. Talijan¹, D. Živković³

¹ University of Belgrade, Institute for Chemistry, Technology and Metallurgy, Njegoševa 12, 11000 Beograd, Serbia

² University of Priština, Faculty of Technical Science, Kos. Mitrovica, Serbia

³ University of Belgrade, Technical Faculty, Bor, Serbia

⁴ University of Kragujevac, Machinery Faculty, Kraljevo, Serbia

Received 7 September 2011, received in revised form 28 September 2011, accepted 30 September 2011

Abstract

Considering the importance of the lead-free solders, alloys of ternary Bi-Sb-Zn system were characterized by microstructural SEM-EDS and optical microscopy analysis, Brinell hardness tests and electrical conductivity measurements. Isothermal cross section at 298 K was calculated using CALPHAD method and PANDAT 8.1 software package. The phases on calculated cross sections were found to be in a good agreement with experimentally determined phase compositions in analyzed microstructures.

Key words: Bi-Sb-Zn system, isothermal section, microstructure, Brinell hardness, electrical conductivity

1. Introduction

Taking into account environmental and health concerns, the intensive investigations of alternative solder alloys to replace conventional lead-tin solders, are still in progress. Given that the Bi-Sb-Zn ternary system is considered as one of the alternative lead-free systems and that zinc alloys, mainly bismuth and antimony doped, are precursors of semiconductors ceramics, it has been widely studied. Majority of papers found in literature are thermodynamic studies and studies of miscibility gap of binary Bi-Sb [1, 2], Bi-Zn and Sb-Zn [3, 4] systems as well as ternary Bi-Sb-Zn system [5, 6]. In our previous work [7] we experimentally and analytically investigated phase diagram of the ternary Bi-Sb-Zn system and three vertical sections of the Bi-Sb-Zn ternary system with molar ratios Bi : Sb = 1, Bi : Zn = 1 and Sb : Zn = 1. The liquidus projection, invariant equilibria, several vertical sections, and an isothermal section at 300°C have been predicted using CALPHAD method. Taking into consideration the possible applications, we broadened our study to electrical and mechanical properties of the alloys from

the three vertical sections of ternary Bi-Sb-Zn system. Furthermore, isothermal section of the Bi-Sb-Zn ternary system at 298 K was predicted using CALPHAD method and compared to the experimentally analyzed microstructures and phase composition of the selected alloys.

2. Experimental procedure

Investigated alloy samples were prepared from high-purity (99.999 mass%) bismuth, antimony and zinc powders produced by Alfa Aesar (Germany). The alloy samples weighing 4 g were prepared in inductive furnace under argon atmosphere and subsequently cooled in air. The samples used for light microscopy, electrical conductivity measurements and hardness tests were prepared by classical metallographic procedure without etching, while the alloy samples used for SEM-EDS analysis were not sealed in polymer. Microstructural analysis was carried out by Scanning Electron Microscopy using JEOL (JSM6460) microscope equipped with Oxford Instruments Energy

*Corresponding author: tel./fax: +381113370412; e-mail address: vlada@tmf.bg.ac.rs

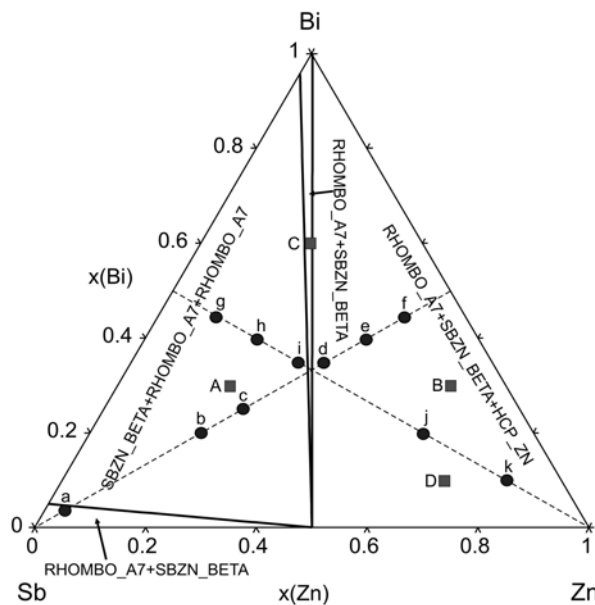


Fig. 1. Isothermal sections in ternary Bi-Sb-Zn system at 298 K.

Table 1. Considered phases, phase's name in the thermodynamic database and Pearson's symbols

Phase common names	Thermodynamic database name	Pearson's symbol
L	LIQUID	
(Bi, Sb)	RHOMBO_A7	hR2
(Zn)	HCP_ZN	hP2
β	SBZN_BETA	oP16
δ	SBZN_DELTA	—
ϵ	SBZN_EPSILON	—
η	SBZN_ETA	oP30
ζ	SBZN_ZETA	oL*
γ	SBZN_GAMMA	—

Dispersive Spectrometer and by light microscopy using OLYMPUS GX41 inverted metallographic microscope. Hardness of the selected samples was determined using HL-400DL impact hardness tester. Electrical conductivity measurements were carried out using Foerster SIGMATEST 2.069 eddy current instrument.

3. Results and discussion

Isothermal section of the Bi-Sb-Zn ternary system at 298 K (Fig. 1) was calculated by CALPHAD method [8, 9] using thermodynamic parameters for constitutive binary systems included in COST 531 [10] database. Names of the considered phases from con-

stitutive binary subsystems, their names in COST 531 database and corresponding Pearson's symbols [11] are listed in Table 1.

Two larger three-phase regions (RHOMBO_A7 + SBZN_BETA + HCP_ZN and SBZN_BETA + RHOMBO_A7 + RHOMBO_A7) and two smaller two-phase regions (RHOMBO_A7 + SBZN_BETA) can be observed in Fig. 1, where in one region RHOMBO_A7 represents (Sb) and in the other (Bi).

3.1. Microstructure analysis

For better insight into possible microstructures of the alloys from ternary Bi-Sb-Zn system eleven microstructures within two vertical sections (BiSb-Zn and BiZn-Sb) are presented in this paper. Compositions of the alloys analyzed using (●) light and (■) scanning electron microscopy (SEM) are marked in Fig. 1, which illustrates calculated isothermal section at 298 K. Analyzed microstructures are presented in Fig. 2.

Microstructure presented in Fig. 2a corresponds to the alloy from two-phase region (RHOMBO_A7 + SBZN_BETA), as it is clearly illustrated. On the other hand, microstructures presented in Fig. 2b,c,g,h,i correspond to the alloys from three-phase region (SBZN_BETA + RHOMBO_A7 + RHOMBO_A7) and the presence of three phases can be observed. Other considered alloys are from the second three-phase region (RHOMBO_A7 + SBZN_BETA + HCP_ZN) consisting of two Bi-rich and Zn-rich solid solutions and one antimony-zinc intermetallic compound.

For the alloys analyzed using SEM, phases that are present in the microstructures were defined by EDS point analysis. Three points were analyzed for each observed phase. Obtained micrographs with marked constitutional phases are presented in Fig. 3, while compositions of the investigated alloys, as above-mentioned, are marked in Fig. 1.

Comparative presentation of the chemical compositions of all four investigated samples, phase compositions as well as calculated and experimentally determined chemical compositions of the present phases is given in Table 2. Experimentally obtained values, presented in Table 2, represent average values based on three measurements.

Comparing the microstructures from Fig. 3 and data from Table 2, good agreement between calculated and experimentally obtained results can be observed.

3.2. Electrical conductivity

Electrical conductivity (σ) of the ternary Bi-Sb-Zn system was investigated within three isothermal sections: BiSb-Zn, BiZn-Sb and SbZn-Bi. Compositions of the referring alloys and their electrical conductivities are given in Table 3. Graphical presentation of the

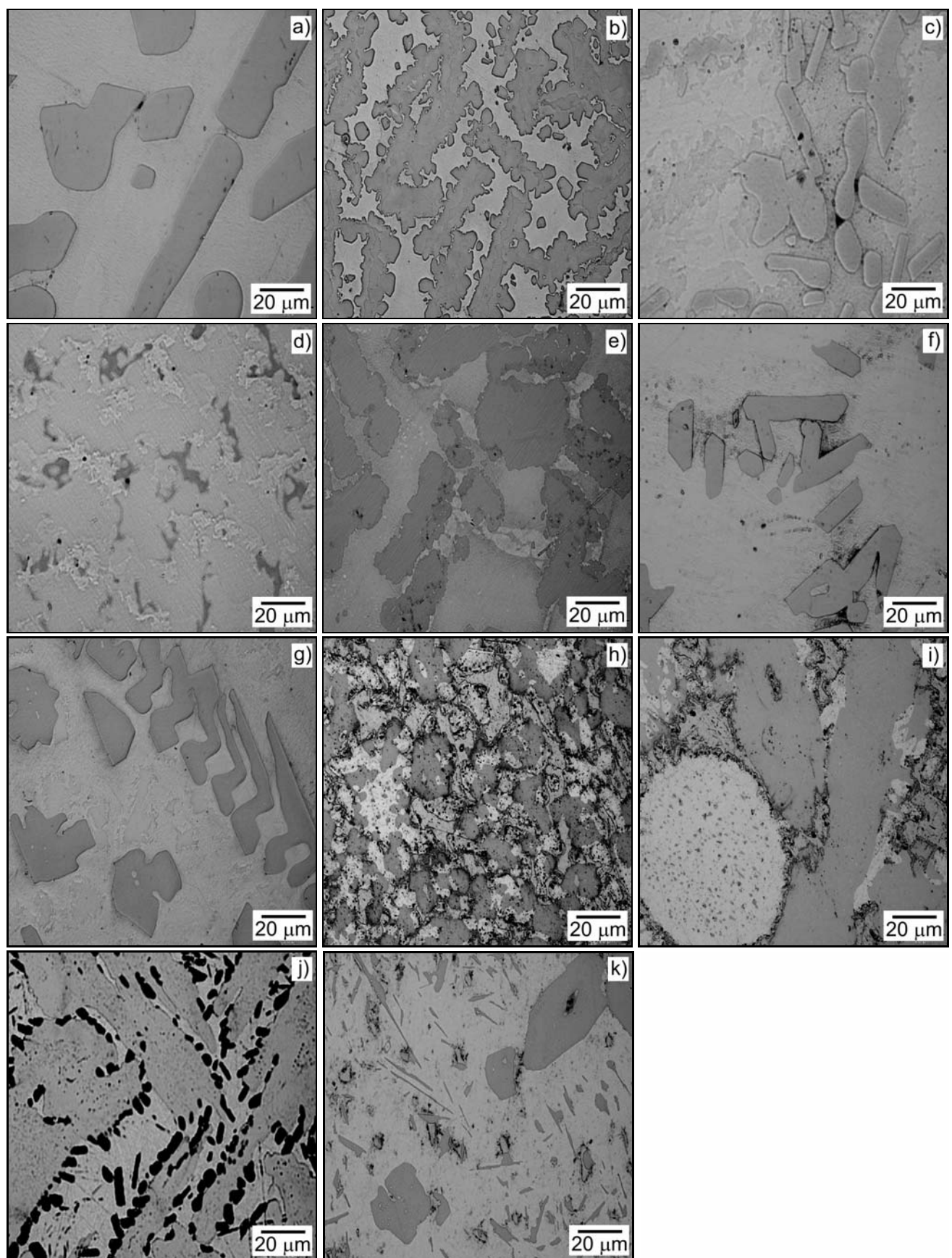


Fig. 2a–k. Microstructures of the alloys of ternary Bi-Sb-Zn system.

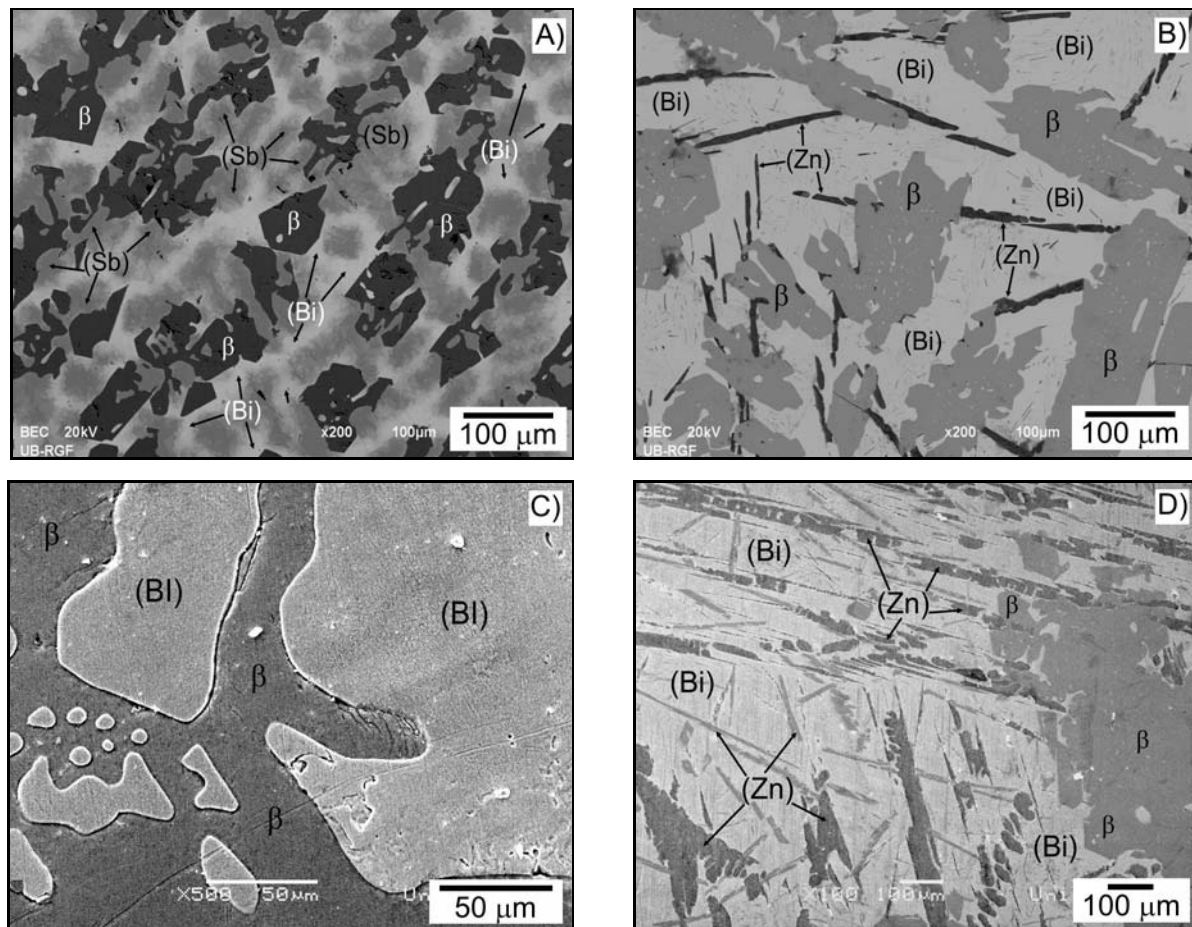


Fig. 3. SEM micrographs illustrating microstructures of the investigated alloys.

Table 2. Calculated and experimentally determined phase compositions in the ternary Bi-Sb-Zn system at 298 K

Alloy	Sample composition (at.%)	Experimentally determined phases	Bi (at.%)		Sb (at.%)		Zn (at.%)	
			exp.	calc.	exp.	calc.	exp.	calc.
I	Bi = 30.7	(Sb)	7.09	4.88	92.91	95.12	—	—
	Sb = 49.3	(Bi)	94.91	95.21	5.09	4.79	48.42	50.23
	Zn = 20	β	—	—	51.58	49.77		
II	Bi = 30.2	(Zn)	1.59	—	1.38	—	97.03	100
	Sb = 9.2	(Bi)	96.31	99.82	2.25	—	1.44	0.18
	Zn = 60.6	β	0.88	—	44.68	49.77	54.45	50.23
III	Bi = 60	(Bi)	96.47	98.03	1.68	1.96	1.85	—
	Sb = 19.6	β	0.48	—	48.62	49.77	50.9	50.23
	Zn = 20.4							
IV	Bi = 10.5	(Zn)	1.24	—	0.96	—	97.8	100
	Sb = 19.2	(Bi)	98.76	99.82	1.08	—	0.14	0.18
	Zn = 70.3	β	0.58	—	50.24	49.77	49.18	50.23

relation between electrical conductivity and molar ratio of the alloys is presented in Fig. 4.

From Fig. 4 it is evident that electrical conductivity of the alloys from all three vertical sections changes

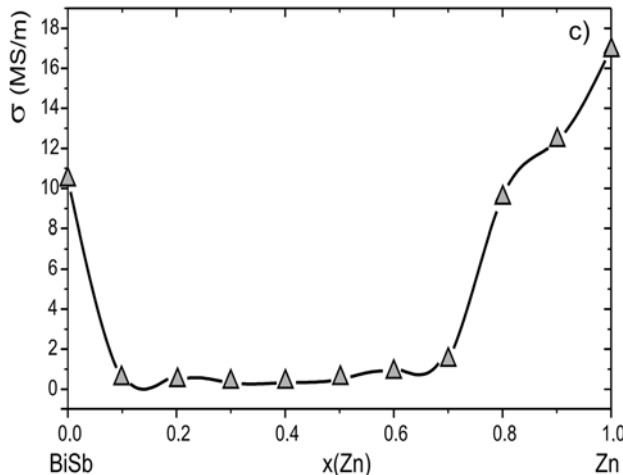
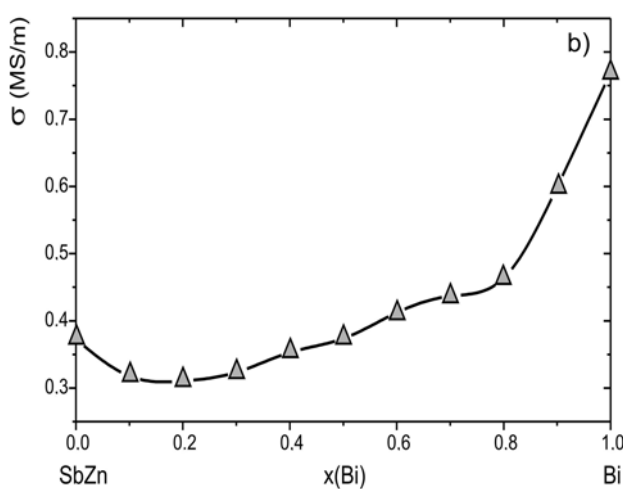
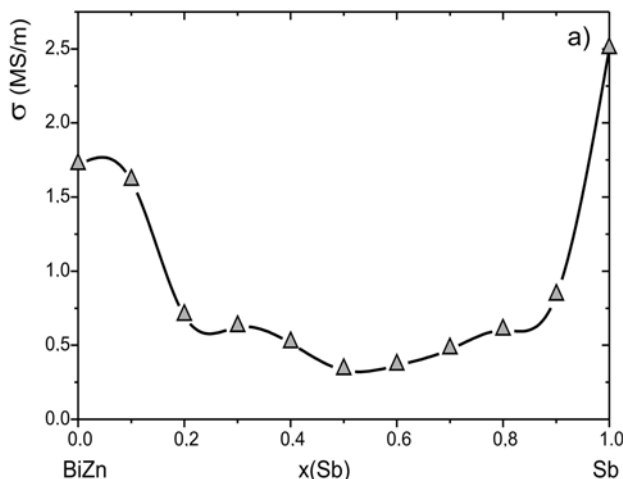


Fig. 4. Electrical conductivity of ternary Bi-Sb-Zn system:
a) vertical BiZn-Sb section, b) vertical SbZn-Bi section and
c) vertical BiSb-Zn section.

in similar manner. From 0 to 0.2 mole fraction of any constitute metal electrical conductivity decreases.

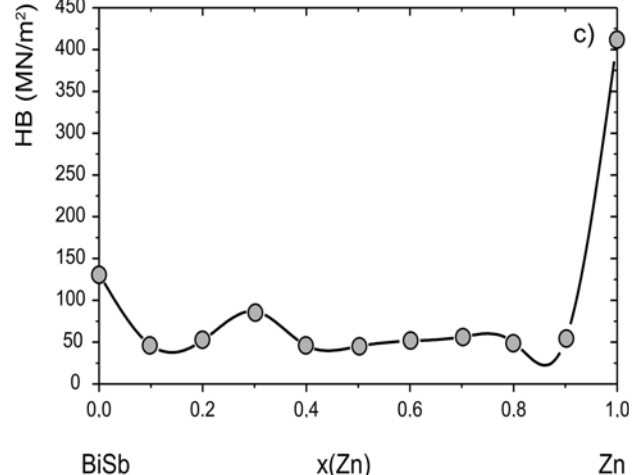
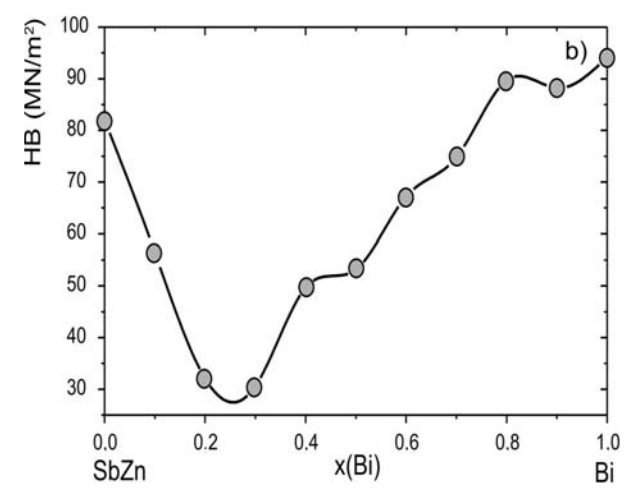
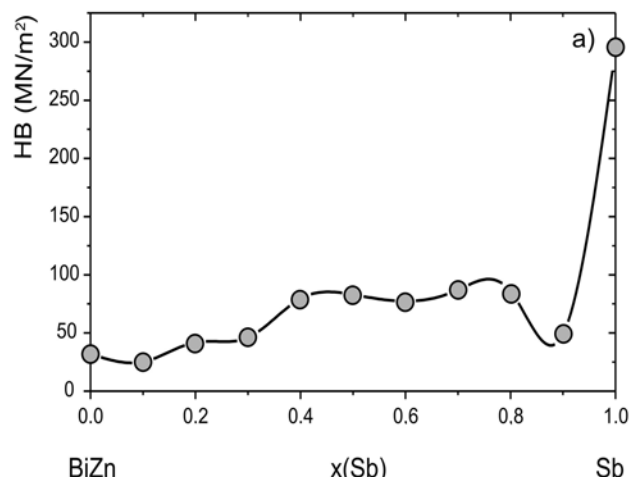


Fig. 5. Brinell hardness of alloys along vertical sections of ternary Bi-Sb-Zn system: a) BiZn-Sb, b) SbZn-Bi and c) BiSb-Zn.

However, this decrease is slightly lower for SbZn-Bi vertical section. From 0.2 until 0.8 mole fraction values

Table 3. Alloys compositions and corresponding electrical conductivities

Alloy composition	Electrical conductivity, σ (MS m^{-1})			
	Measurement 1	Measurement 2	Measurement 3	Average value
$x(\text{Bi})$	Bi-SbZn			
0	0.3726	0.3753	0.3843	0.3774
0.1	0.318	0.3153	0.3117	0.315
0.2	0.3102	0.3078	0.3088	0.3089
0.3	0.3233	0.3215	0.3307	0.3251
0.4	0.3527	0.3546	0.3523	0.3532
0.5	0.3739	0.3718	0.3736	0.3731
0.6	0.412	0.4156	0.4134	0.4136
0.7	0.4367	0.4451	0.4462	0.4426
0.8	0.4635	0.4589	0.4996	0.474
0.9	0.5982	0.6123	0.5987	0.603
1.0	0.77	0.77	0.77	0.77
$x(\text{Zn})$	Zn-BiSb			
0	10.46	10.47	10.68	10.5366
0.1	0.479	0.473	0.483	0.4783
0.2	0.3948	0.473	0.391	0.4196
0.3	0.3218	0.297	0.326	0.3149
0.4	0.3235	0.3226	0.3215	0.3225
0.5	0.493	0.592	0.4859	0.5236
0.6	0.8325	0.8599	0.8632	0.8518
0.7	1.443	1.516	1.347	1.4353
0.8	9.599	9.547	9.949	9.6983
0.9	1212.352	11.985	12.574	12.3036
1.0	17	17	17	17
$x(\text{Ag})$	Sb-BiZn			
0	1.7256	1.7143	1.7167	1.7188
0.1	1.612	1.605	1.61	1.609
0.2	0.678	0.684	0.698	0.6866
0.3	0.6142	0.6123	0.6212	0.6159
0.4	0.5233	0.5187	0.5134	0.5184
0.5	0.3346	0.3357	0.3318	0.334
0.6	0.3823	0.3735	0.3629	0.3729
0.7	0.472	0.4747	0.4716	0.4727
0.8	0.5972	0.603	0.5997	0.5999
0.9	0.695	0.795	0.8339	0.7746
1.0	2.5	2.5	2.5	2.5

of electrical conductivity are virtually constant and furthermore above 0.8 mole fraction they increase significantly.

3.3. Mechanical properties

Hardness of the investigated alloys within the three vertical sections: Sb-BiZn, Bi-SbZn and Zn-BiSb was determined using Brinell test method. Compositions of the investigated alloys and experimentally determined hardness are given in Table 4. Graphical representation of the dependence of hardness vs. molar ratio within the considered vertical sections is presented in Fig. 5.

In general, obtained results (Table 4, Fig. 5) illustrate an increase of hardness in all three quasi-binary sections with increasing molar ratio of corresponding metal. Nevertheless, more modest increase can be observed for BiSb-Zn section.

4. Conclusion

By using thermodynamic parameters from literature isothermal section at 298 K has been calculated by CALPHAD method. It was found to have two two-phase regions and two three-phase regions. Compared to the results of the microstructural ana-

Table 4. Alloys compositions and Brinell hardness

Sb-BiZn		Bi-SbZn		Zn-BiSb	
$x(\text{Sb})$	HB (MN m ⁻²)	$x(\text{Bi})$	HB (MN m ⁻²)	$x(\text{Zn})$	HB (MN m ⁻²)
0	132	0	32	0	82
0.1	46	0.1	25.3	0.1	56.4
0.2	52	0.2	42	0.2	32.1
0.3	87	0.3	46	0.3	30.6
0.4	45.9	0.4	79.6	0.4	49.7
0.5	45	0.5	83	0.5	53.2
0.6	51.5	0.6	77.3	0.6	67.2
0.7	56.1	0.7	87	0.7	74.8
0.8	49.7	0.8	85.7	0.8	89.7
0.9	52	0.9	48.6	0.9	88.2
1	412	1	294	1	94.2

lysis by optical microscopy and SEM-EDS analysis it shows good correspondence of the calculated number and chemical composition of phases. Brinell hardness and electrical conductivity were experimentally determined for the selected alloys from three vertical sections of ternary Bi-Sb-Zn system. Although initially there are differences in how electrical conductivity and hardness of the investigated alloys change with the increase of the molar ratio of corresponding metal, above 0.8 mole fraction they both increase significantly.

Acknowledgements

The financial support of the Ministry of Education and Science of the Republic of Serbia under the Project ON 172037 is acknowledged. The results of this paper are also in the frame of the project COST MP0602. Calculations were performed using Pandat 8.1 software.

References

- [1] Feutelais, Y., Morgant, G., Didry, J. R., Schnitter, J.: CALPHAD, 16, 1992, p. 111.
[doi:10.1016/0364-5916\(92\)90001-E](https://doi.org/10.1016/0364-5916(92)90001-E)
- [2] Ohtani, H., Ishida, K.: J. Electron. Mater., 23, 1994, p. 747. [doi:10.1007/BF02651369](https://doi.org/10.1007/BF02651369)
- [3] Adjadj, F., Belbacha, E. D., Bouharkat, M., Kerboub, A.: J. Alloys Compd., 419, 2006, p. 267.
[doi:10.1016/j.jallcom.2005.09.068](https://doi.org/10.1016/j.jallcom.2005.09.068)
- [4] Adjadj, F., Belbacha, E. D., Bouharkat, M.: J. Alloys Compd., 430, 2007, p. 85.
[doi:10.1016/j.jallcom.2006.04.051](https://doi.org/10.1016/j.jallcom.2006.04.051)
- [5] Bouharkat, F., Couniou, J. J., Vignalou, J. R., Said, J.: J. Alloys Compd., 238, 1996, p. 149.
[doi:10.1016/0925-8388\(95\)02095-0](https://doi.org/10.1016/0925-8388(95)02095-0)
- [6] Bouharkat, M., Adjadj, F.: Journal of Phase Equilibria and Diffusion, 32, 2011, p. 279.
[doi:10.1007/s11669-011-9902-1](https://doi.org/10.1007/s11669-011-9902-1)
- [7] Minić, D., Dokić, J., Čosović, V., Stajić-Trošić, J., Živković, D., Dervišević, I.: Mater. Chem. Phys., 122, 2010, p. 108. [doi:10.1016/j.matchemphys.2010.02.078](https://doi.org/10.1016/j.matchemphys.2010.02.078)
- [8] Saunders, N., Miodownik, A. P.: CALPHAD (A Comprehensive Guide). London, Elsevier 1998.
- [9] Lukas, H. L., Fries, S. G., Sundman, B.: Computational Thermodynamics: The CALPHAD Method. Cambridge, Cambridge University Press 2007.
[doi:10.1017/CBO9780511804137](https://doi.org/10.1017/CBO9780511804137)
- [10] Dinsdale, A. T., Kroupa, A., Vízdal, J., Vřeštál, J., Watson, A., Zemanová, A.: COST Action 531 – Database for Lead-free Solders, Ver. 3.0, 2008 (unpublished research).
- [11] Dinsdale, A. T., Watson, A., Kroupa, A., Vřeštál, J., Zemanová, A., Vízdal, J. (Eds.): COST Action 531 – Atlas of Lead Free Soldering, Volume 1, Belgium, COST Office 2008.